

Experimental calibration of numerical models for short coupling beams of a multi-story frame structure



F. Dinu, D. Dubina

*Politehnica University of Timisoara, Romania
Romanian Academy, Timisoara Branch*

C. Neagu & C. Vulcu

Politehnica University of Timisoara, Romania

D. Marcu

*„Ion Mincu” University of Architecture and Urbanism, Bucharest, Romania
Popp & Associates Ltd, Bucharest, Romania*

SUMMARY:

Beams with span-to-depth ratio shorter than four are not very common in the design of moment resisting frames. For such beams, the shear stresses may become a controlling factor in the design. The current design procedure results in an over design for bending capacity and under design for shear resistance. This is a very important issue when the beam is part of the seismic lateral resisting system, designed according to the dissipative concept. In this case, the presence of shear force affects the dissipation capacity and plastic mechanism. The paper presents the calibration of a numerical model for short beams based on experimental test on full scale specimens. A reduced beam section connection is employed for beam-to-column connection. The study is connected with the design of a 18-story office building.

Keywords: reduced beam section, numerical model, experimental test, short beam, steel moment frames

1. INTRODUCTION

Moment resisting frames are often used as part of the seismic force resisting systems, due to their inherent ductility. Inelastic behavior is intended to be accommodated through plastic hinges in beams near the beam-to-column connections, and also at column bases. Even considered deemed-to-comply connections, welded beam-to-column connections experienced serious damage and even failures during strong seismic events. These failures included fractures of the beam flange-to-column flange groove welds, cracks in beam flanges, and cracks through the column section (FEMA 350, 2000). One way of reducing the risk of brittle failure of such connections is by either connection strengthening (Figure 1.a) or beam weakening (Figure 1.b). First approach consists in providing sufficient overstrength to connection, for example by means of haunches or cover plates. Because of material overstrength and strain hardening effects, the design forces and bending moments in the connections can be substantially large. The other possibility to avoid brittle fracture of the beam-to-column connection is the weakening of the beam near the beam ends. One example is the "Reduced Beam Section" (RBS) or "dog-bone" concept. This was initially proposed by Plumier (1990) and then developed and patented by ARBED, a Luxembourg-based steel manufacturing company. ARBED waived in 1995 all patent and claim rights associated with the RBS. Proper detailing of the reduced beam section, including flange cutouts and beam to column welding is needed to ensure the formation of plastic hinges in the reduced zones.

It is economical to keep the width of bays in some limits, because long bays make the structure flexible and therefore increase the drift, which may control the design. On the other hand, short bays can cause a reduction of the dissipation capacity due to the presence of large shear forces. The design rules for interaction between shear force and bending moment can be found in EN 1993-1-1 (2005) for class 1 and 2 sections and in EN 1993-1-5 (2006) for class 3 and 4 sections (B. Johansson et al., 2007). The interaction formula in EN 1993-1-1 starts the reduction of bending resistance when shear force is larger than the plastic shear resistance, $V > 0.5V_{pl}$. The same limitation is given in EN 1998-1 (2004),

for dissipative moment of moment frames. As a result, the connection qualification specifies minimum span-to-depth ratio to be used for moment frame connections. When prequalified connections are utilized outside the parametric limitations, project specific qualification must be performed to permit the prediction of behavior and acceptance criteria (FEMA 350, 2000).

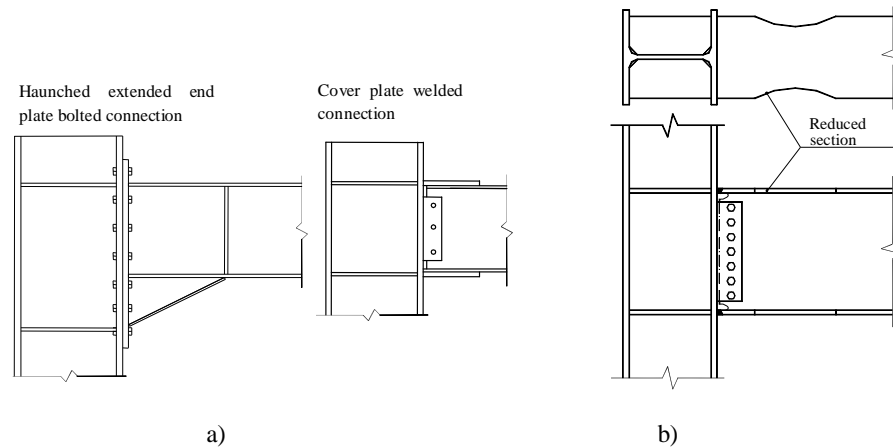


Figure 1. Reducing stress concentration in connections: a) connection strengthening; b) beam weakening using reduced beam section concept

This paper presents part of a research project that was performed to check the validity of the moment frame connections of a 18-story steel frame building. The building owner is DMA Architecture & Interior Design, Bucharest, Romania. The structural analysis and design was done by Popp & Associates, a design and consulting office based in Bucharest, Romania.

The paper describes the calibration of numerical models for two types of reduced beam section connections using the general-purpose finite element analysis program ABAQUS (2007). The finite element models were calibrated using experimental tests performed on four full-scale specimens at the Laboratory of Steel Structure, "Politehnica" University of Timisoara, Romania. The particularity of the project consists of very short bay widths coupled with the use of reduced beam section connections for the moment frame connections. In addition, the project incorporates flush-end plate bolted connections for beam splices and therefore the study addresses concerns regarding the potential for brittle failure of the bolts.

2. TEST PROGRAM

The study is connected with the design of a 18-story office building, located in Bucharest, Romania. The building height is 94 m, and the plan dimensions are 43,3m x 31,3m, see Figure 2. The building site is located in a high seismic area, which is characterized by a design peak ground acceleration 0.24g for a returning period of 100 years, and soft soil conditions, with $T_c=1.6$ s. It is noteworthy the long corner period of the soil, which in this case may affect flexible structures. For serviceability check, the returning period is 30 years, while for collapse prevention it is 475 years.

Lateral force-resisting system consists of exterior steel framing with closely spaced columns and short beams. The central core is also made of steel framing with closely spaced columns and short beams. The ratio of beam length-to-beam height, L/h , varies from 3.2 to 7.4, which results in seven different types of beams. Some beams are below the general accepted inferior limit ($L/h=4$). The moment frame connections employ reduced beam section connections that are generally used for beams loaded mainly in bending (Figure 3). Circular radius cuts in both top and bottom flanges of the beam were used to reduce the flange area. The detailing followed the recommendations contained in FEMA 350. Welds of beam flanges and web to column flange are complete joint penetration groove welds. Two types of beams, which have the shortest L/h ratio, have been selected for the experimental program. Table 1 shows the characteristics of the beams tested experimentally. The first beam, denoted as RBS-S, has a clear length of 1450 mm, and the lowest span over height ratio, $L/h=3.2$. The second type,

denoted as RBS-L, has a clear length of 2210 mm, and a corresponding span over height ratio L/h of 4.9 (Figure 3). The thickness of the web and flanges for both beam types is 20 mm and 14 mm, respectively. Bolted flush endplate slip resistant connections were adopted for the splice beam connection. The column has a cruciform cross-section made from two hot-rolled profiles of HEA800 and HEA400 section.



Figure 2. Plan layout and elevation of the building

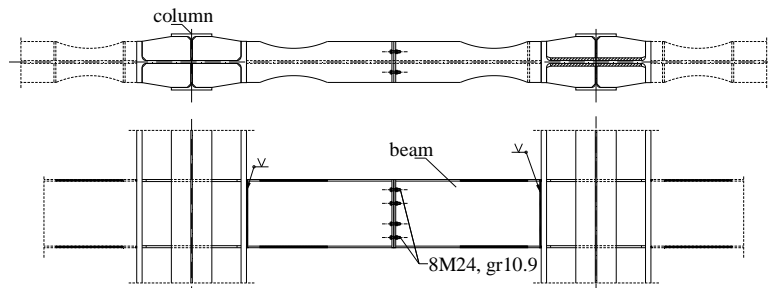


Figure 3. Reduced beam section connection

Table 1. Characteristics of beams tested experimentally

Type	h [mm]	b [mm]	L [mm]	W [mm ³]*10 ³	A_v [mm ²]*10 ²	f_y [N/mm ²]	M_p [KNm]	V_p [KN]	M_p/V_p	L/h	$L/[M_p/V_p]$
RBS-S	450	250	1450	1806	90	355	641	1845	0.35	3.2	4.17
RBS-L	450	250	2210	1806	90	355	641	1845	0.35	4.9	6.36

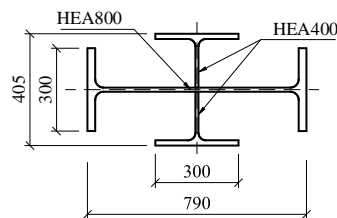


Figure 4. Cruciform cross-section of the columns

Both beams and columns are made from S355 grade steel. The base material characteristics have been evaluated experimentally. The actual (measured) yield strength of the plates and profiles were larger than the nominal values. The highest increase has been recorded for the hot rolled profiles, while the plates shown a smaller increase. This increase is the material overstrength factor, and is limited to 1.25 in seismic code EN1998-1 (2004).

Table 2. Material properties of hot rolled profiles

Section	Steel grade	Element	f_y	f_u	A_u
HEA800	S355	Flange	410.5	618.5	18.0
		Web	479.0	671.2	19.0
HEA400	S355	Flange	428.0	592.0	18.1
		Web	461.0	614.0	17.8

Table 3. Material properties of flat steel

Section	Steel grade	Element	f_y	f_u	A_u
14 mm	S355	Beam flange	373.0	643	18.0
20 mm	S355	Beam web	403.0	599	17.5

Figure 5 shows the test setup. The lateral loading was applied quasi-static under displacement control. Specimens were tested under cyclic loading. The cyclic loading sequence was taken from the ECCS Recommendations (ECCS, 1986). Thus, according to the ECCS procedure, the yielding displacement D_y and the corresponding yielding force F_y are obtained from the monotonic force vs. displacement relationship using a tangent with 10% of the initial stiffness slope at the maximum force. In order to reduce the number of tests, the monotonic test was replaced by the push-over curve obtained numerically using the general-purpose finite element analysis program ABAQUS. The yielding displacement is then used for establishing the cyclic loading. It consists in generating 4 successive cycles for the ranges of displacement $\pm 0.25D_y$, $\pm 0.5D_y$, $\pm 0.75D_y$, $\pm 1.0D_y$ followed up to failure by series of 3 cycles each with a range $\pm 2n \times D_y$ where n is = 1, 2, 3,.....etc (Figure 6).

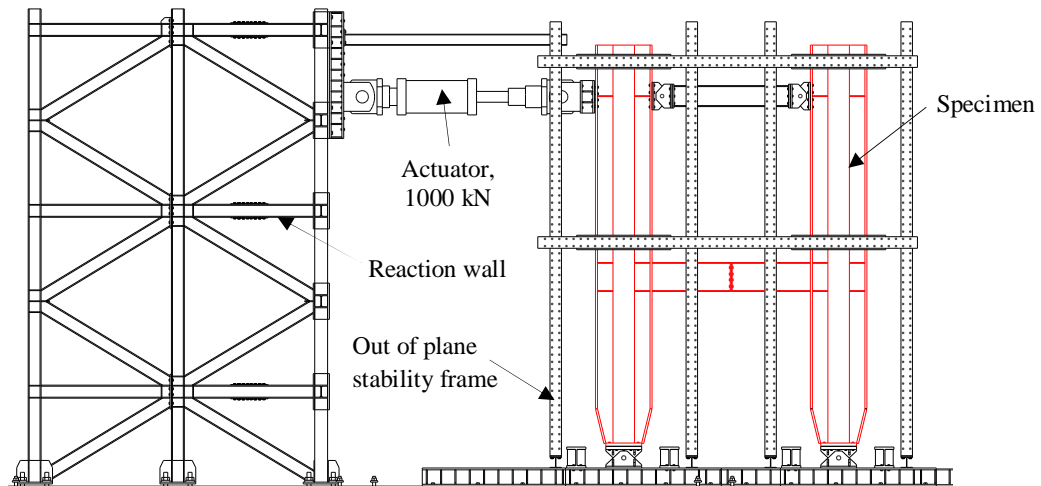


Figure 5. Test set-up

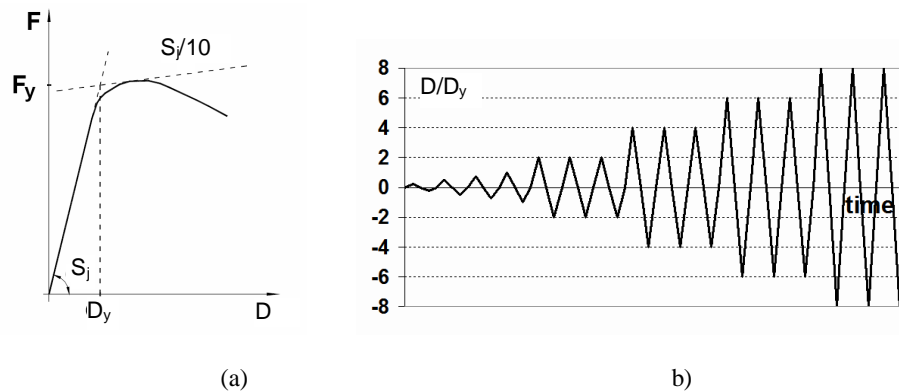
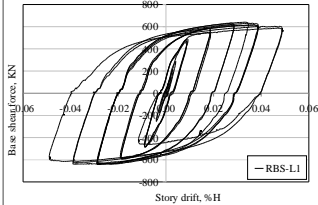
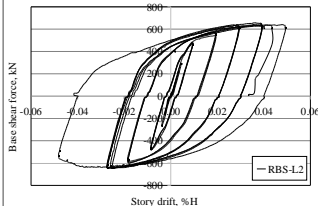
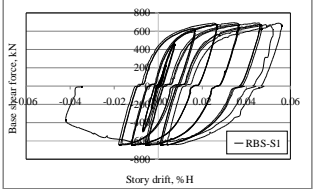
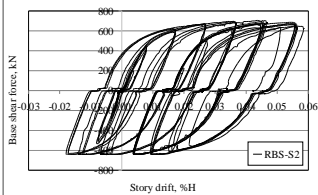


Figure 6. Loading protocol: a) determination of yielding displacement; c) cyclic loading protocol

2.2. Experimental results

Table 4 summarizes the experimental results, with observations regarding the behavior and failure mode of each specimen. Specimens with longer beams, RBS-L1 and RBS-L2, remained elastic until a drift of 30 mm, or 0.6% of the story height. The visible buckling of the flange in compression was first observed, followed by out-of-plane buckling of the web. Two failure modes were recorded. First mode involved fracture of the top beam flange to column flange welding, which also propagated in the web. The second involved the fracture of the bottom flange due to the large tensile forces at ultimate stage. The plastic behavior was dominated by the buckling of the flange in compression and out of plane buckling of the web. Specimens with shorter beams, RBS-S1 and RBS-S2, remained elastic until a drift of 25 mm, or 0.5% of the story height. The visible buckling of the flange in compression was first observed, followed by out-of-plane buckling of the web. Failure of the first short specimen, RBS-S1, involved fracture of the bottom flange due to the large tensile forces at ultimate stage, followed then by the fracture of the lower half of the web. The failure of the second specimen, RBS-S2, involved the fracture of the bolts at the splice connection. The plastic behavior was dominated by the buckling of the flange in compression and shear buckling of the web. Both types of specimens failed at interstory drifts larger than 5% of the story height. This capacity supports the design of the structure which is based on a 2.5% interstory drift at the Ultimate Limit State.

Table 4. Results of experimental tests

Specimen	Failure mode	Details: failure mode and force-displacement curve		Observations
RBS-L1	- cracks initiated in top flange to column welding, fracture propagated in web			- failure at interstory drift of 5% - no slip at splice connection - large dissipation capacity, reduce cyclic degradation
RBS-L2	- failure due to fracture of the flange in the reduced area, then propagation in the web			- failure at interstory drift of 5% - no slip at splice connection - large dissipation capacity, reduce cyclic degradation
RBS-S1	- failure due to fracture of the flange in the reduced area, then propagation in the web			- failure at interstory drift of 5% - moderate slip at splice connection - large dissipation capacity, reduced cyclic degradation
RBS-S2	- failure due to fracture of the bolts at beam splice connection			- failure at large interstory drift - large slip at splice connection - large dissipation capacity, reduced cyclic degradation

The optical measuring device VIC-3D was used to measure the out of plane deformations of the web within an area of 450×550 mm centered in the reduced beam section zone. The three-dimensional video image correlation system (VIC-3D) is a displacement and strain measurement technique developed by Correlated Solutions, Inc. and uses a mathematical correlation method to analyze digital image data taken while a test specimen is subjected to load. The system has a point-to-point strain accuracy of 0.02% and therefore can provide accurate measurements regarding the object contour and

out-of-plane displacements of the infill panel on the highlighted area. Figure 7 and Figure 8 show the evolution of web out of plane plastic deformations in the zone adjacent to the column. Under the increasing lateral force, the plastic mechanism in the web involves both bending moment and shear force. The contribution from the shear force to the overall deformation is more important for the short specimens, RBS-S, and this is evidenced by the inclination of the buckled shape of the web.

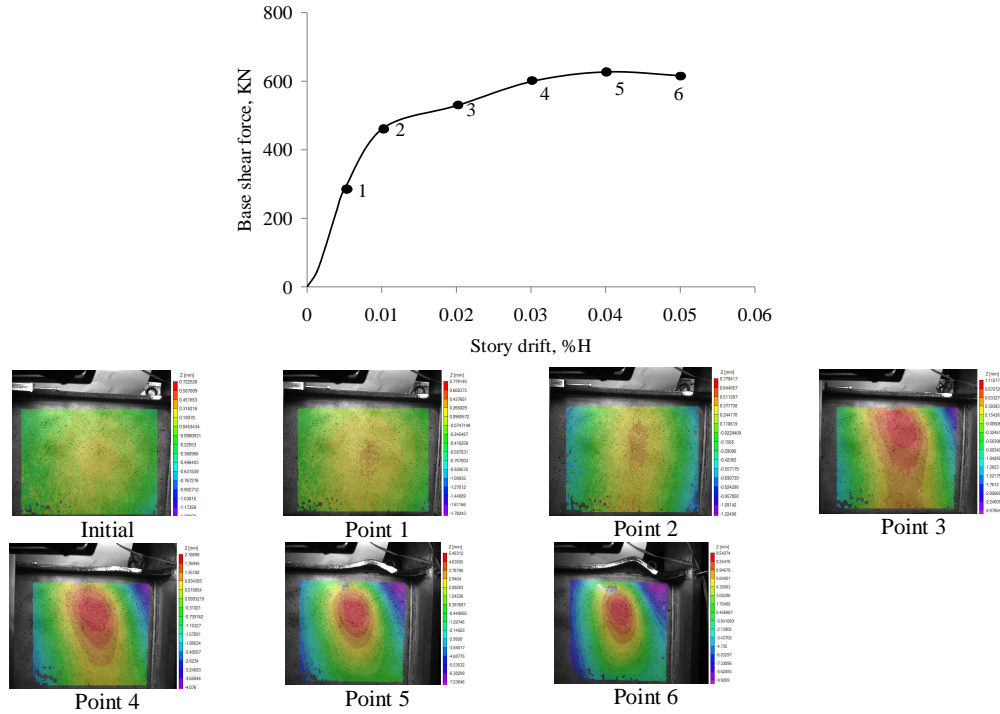


Figure 7. VIC measurements with the scale on the right, RBS-L1

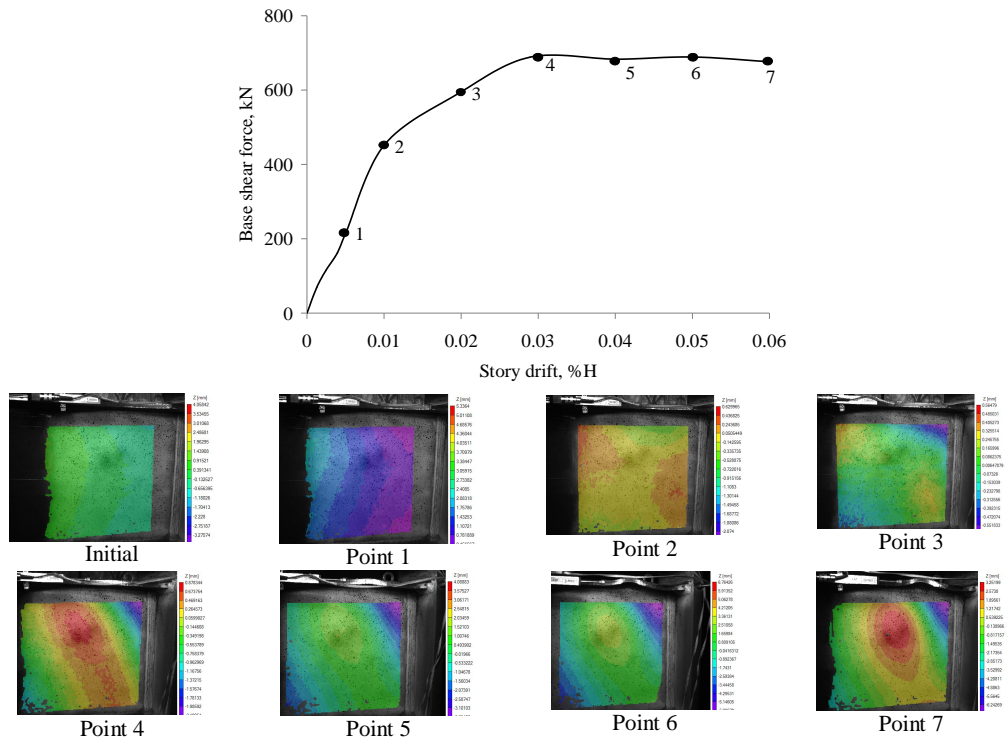


Figure 8. VIC measurements with the scale on the right, RBS-S2

Figure 9 shows the moment-rotation curve for all specimens. The total rotation of the joint has two major components: rotation of the beam (reduced beam section) and distortion of the web panel in the reduced region. Due to the large stiffness of the columns, the contribution of the column web panel can be neglected. The specimens exhibited stable hysteretic behavior and good rotation capacity. The specimens showed a limited degradation of strength and stiffness. The bolts slip during testing of short specimens, and this is clearly indicated by the shape of the hysteretic curves (Figure 9).

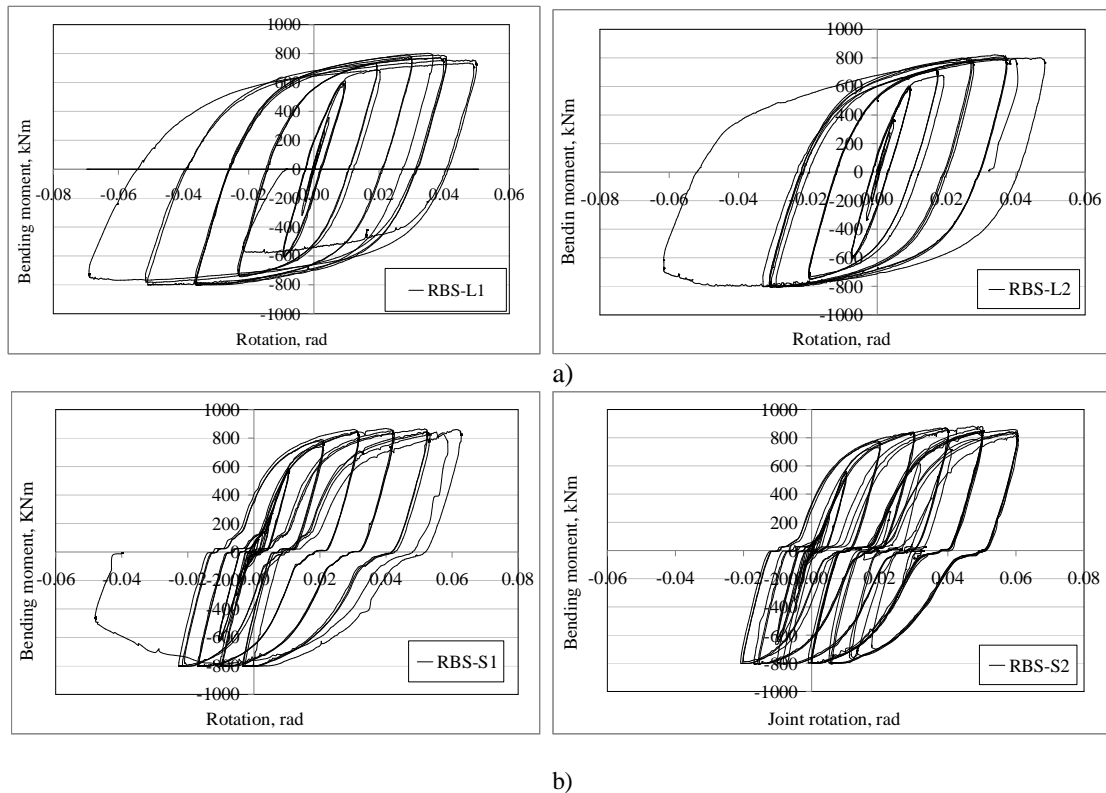


Figure 9. Moment-rotation relationship for cyclic loaded joints: (a) RBS-L specimens; (b) RBS-S specimens

3. NUMERICAL INVESTIGATION

3.1. Description of the numerical model

A set of numerical simulations have been performed with the finite element modeling software ABAQUS (2007). All the components were modeled using solid elements. In order to have a uniform and structured mesh, some components with a complex geometry were partitioned into simple shapes. The following parts of the joint configurations were used in the numerical models:

- Steel columns, made of cruciform section HEA800-HEA400, S355 grade steel
- Beams made from welded steel plates, S355 grade steel
- Stiffeners, S355 grade steel
- End plates at beam splice connection, S355 grade steel
- Bolts M24, 10.9, used for the beam splice connection.

With the aim to assess the behavior of the beams and the development of plastic hinges, the assembly consists of two columns and two beams, connected at the mid span by means of a flush-end plate bolted connection (Figure 10). Even the splice connection was designed with slip-critical high-strength bolts, in the analysis the bolts were modeled as normal bolts with standard holes. This can be considered conservative because if the bolts slip under extreme loading conditions, the connection should resist the forces between the two parts of the beam. In practical conditions, due to the fabrication and erection tolerances, it is hard to achieve a closed contact between the two end plates. If

additional gusset plates are inserted to cope with the gap between the end plates, this can reduce or minimize the effect of bolts preloading. The engineering stress-strain curves of the steel grades obtained from tensile tests were computed into true stress-true plastic strain and used further in the numerical model. The modulus of elasticity was considered equal to 210000 N/mm^2 and the Poisson coefficient equal to 0.3. A dynamic explicit type of analysis was used. The load was applied through displacement control at the top of the columns (see Figure 11) with pinned connection at the bottom. The mesh of the elements was done using linear hexahedral elements of type C3D8R.

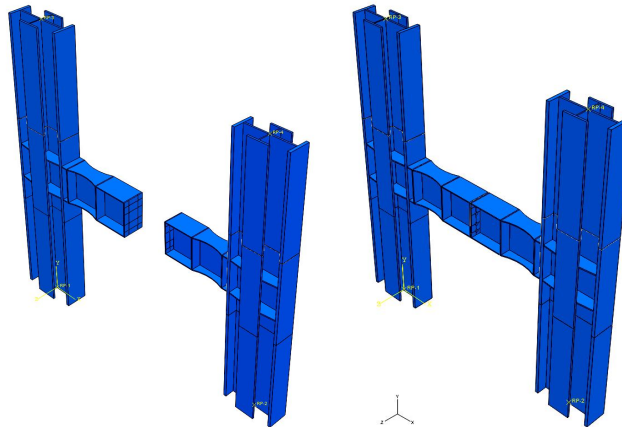


Figure 10. Assembly of the numerical model

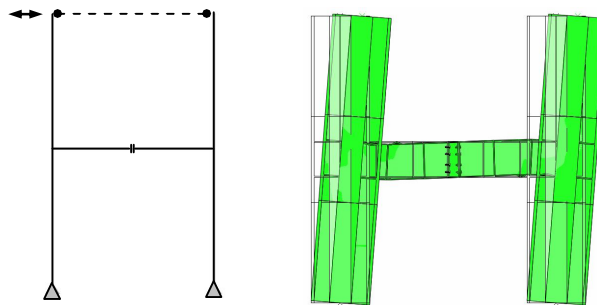


Figure 11. Load application through displacement control

3.2. Analysis of specimens

Figure 12 shows the comparison of the numerical base shear force - top displacement versus the experimental ones. It was found the numerical model can predict with a good accuracy the response of the structure.

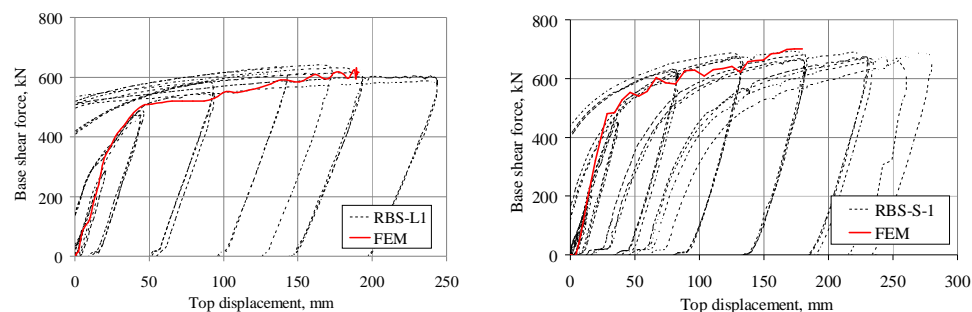


Figure 12. Comparison between experimental and analytical results (only positive range is plotted)

For long specimens, the slip at the splice connection is reduced and does not affect the global behavior during the cyclic loading (Figure 13). The yield force and yield displacement are in good agreement with the experimental values. The post-elastic stiffness approximates very well the envelope curve obtained in the cyclic test. The test on short specimens shown that the shear force increases and, if coupled with lack of contact between the end plates, this may cause the slippage of the two beam segments. This tends to reduce the rigidity under lateral loads and therefore it must be taken into account. Therefore, in the FEM analysis, a gap between the two end plates has been employed (Figure 14, Figure 15). Under large lateral displacements, the slip can cause also the fracture of the bolts. Based on these results, a redesign of the splice connection, which is more consistent with the predominant shear stress at the mid-length of the beams, is proposed. This new connection detail consists of gusset plates on web and flanges and preloaded high strength bolts. The detail should prevent the bolt slippage which can cause both an increase of the lateral deflection and brittle failure of the bolts under large lateral displacements.

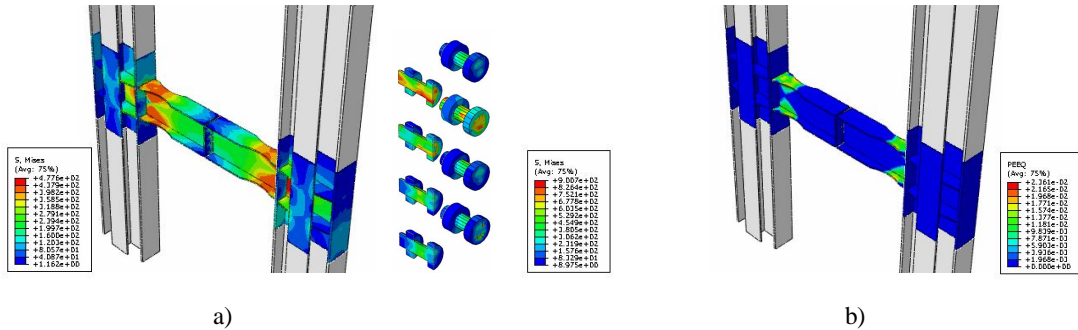


Figure 13. FEM results for long specimen RBS-L1: a) Von Mises stress in members and bolts; b) plastic deformations in beams

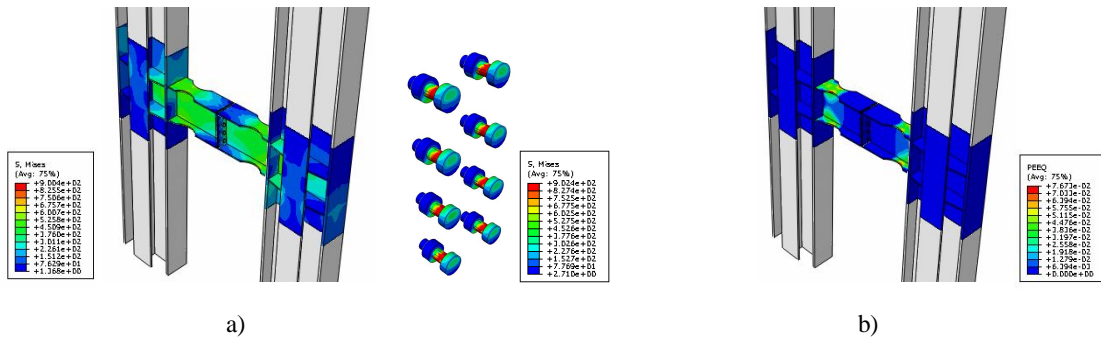


Figure 14. FEM results for short specimen RBS-S1: a) Von Mises stress in members and bolts; b) plastic deformations in beams

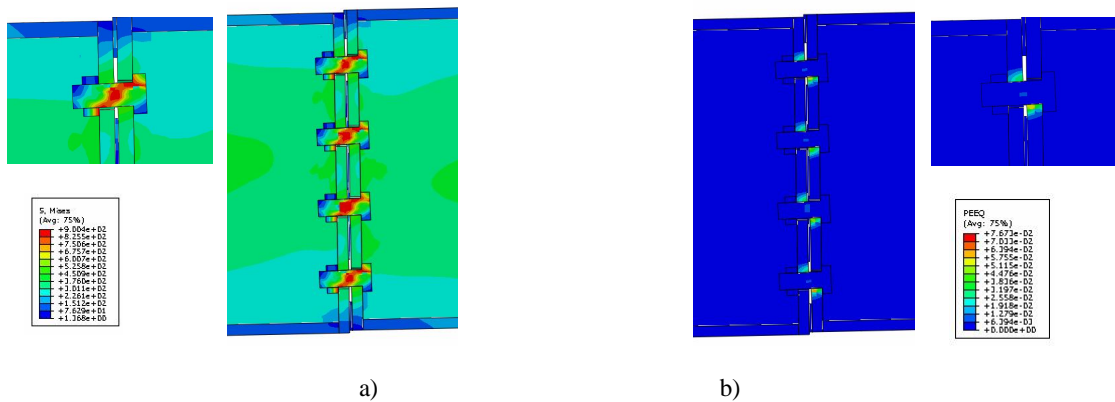


Figure 15. Gap between the end plates for short specimens: a) Von Mises stress; b) plastic deformations

4. CONCLUSIONS

Main conclusions on the experimental tests and numerical analysis of reduced beam sections connections of short coupling beams can be summarized as follows:

- Experimental tests on two types of short beams of RBS connections confirmed the design procedure. The specimens exhibited excellent ductility and rotation capacity up to 60 mrad before failure. The numerical model can predict with a good accuracy the response of the structure if the slippage at the splice connections is appropriately accounted for. Based on the results, a redesign of the splice connection, which is more consistent with the predominant shear stress at the mid-length of the beams, is proposed. This new connection detail consists of gusset plates on web and flanges and preloaded high strength bolts. The detail should prevent the bolt slippage which can cause both an increase of the lateral deflection and, under extreme deformations, brittle failure of the bolts.
- For very short beams, the interaction between the shear and normal stresses caused an inclination of the buckled shape in the web. The plastic rotation capacity has two major components, i.e. rotation of the beam (reduced beam section) and distortion of the web panel in the reduced region. Due to the large stiffness of the columns, the contribution of the column web panel can be neglected.
- Numerical analysis for cyclic loading is in progress. The numerical simulation of the slip behavior will be also considered. The final calibrated model will be applied to verify the design procedure for the types of connections proposed in the project.
- For design purposes, a fiber hinge model of the plastic zone (reduced beam section) will be also developed. The model will be employed in the nonlinear static and dynamic analysis and design of the steel frame building.

ACKNOWLEDGEMENT

Funding of the project was made in the frame of the contract 76/2011 “Numerical simulations and experimental tests on beam-column subassemblies from the structure of a 17 story steel building in Bucharest, Romania” between the “Politehnica” University of Timisoara and DMA ARCHITECTURE & INTERIOR DESIGN LTD, Bucharest, Romania.

C. Vulcu was partially supported by the strategic grant POSDRU/88/1.5/S/50783, Project ID50783 (2009), co-financed by the European Social Fund - Investing in People, within the Sectorial Operational Program “Human Resources Development”, 2007-2013.

REFERENCES

- ABAQUS User’s Manual, Version 6.9 (2007). D. Hibbit, B. Karlson & P. Sorenson, Inc.
- A. Plumier (1990). New Idea for Safe Structures in seismic Zones. IABSE Symposium. Mixed structures including new materials - Brussels 1990.pp. 431 - 436.
- B. Johansson, R. Maquoi, G. Sedlacek, C. Müller, D. Beg (2007). Commentary and worked examples to EN 1993-1-5, JRC – ECCS cooperation agreement for the evolution of Eurocode 3, European Commission.
- EN 1993-1-1 (2005). Eurocode 3. Design of steel structures. General rules and rules for buildings, CEN, EN 1993-1-1.
- EN 1993-1-5 (2006). Eurocode 3. Design of steel structures. Part 1-5: General rules - Plated structural elements, CEN, EN 1993-1-5.
- EN 1998-1 (2004). Design provisions for earthquake resistance of structures - 1-1: General rules - Seismic actions and general requirements for structures, CEN, EN 1998-1.
- European Convention for Constructional Steelwork, Technical Committee 1, Structural Safety and Loadings; Working Group 1.3, Seismic Design (ECCS) (1986). Recommended Testing Procedure for Assessing the Behavior of Structural Steel Elements under Cyclic Loads, First Edition.
- Federal Emergency Management Agency (FEMA 350) (2000). Recommended seismic design criteria for new steel moment-frame buildings. Rep. No. FEMA-350, SAC Joint Venture, Washington, D.C.